

A study of the electrophoretic deposition of bioactive glass–chitosan composite coating

Mehrad Mehdipour^{*}, Abdollah Afshar

Department of Materials and Engineering, Sharif University of Technology, Azadi Avenue, P.O. Box 11155-9466, Tehran, Iran

Received 13 June 2011; received in revised form 13 July 2011; accepted 15 July 2011

Available online 23rd July 2011

Abstract

Bioactive glass is coated on implant's surface to improve corrosion resistance and osseointegration, when placed in the body. Bioactive glass particles were synthesized through a sol–gel process and deposited along with chitosan to form a composite coating on a stainless steel substrate using electrophoretic deposition technique. Stable suspensions of chitosan–bioactive glass were prepared using bioactive glass particles ($<1\ \mu\text{m}$) and 0.5 g/l chitosan solution. The influence of ethanol–water ratio on deposition yield was investigated. For all process conditions, best results were achieved with suspension of 30 vol% water in ethanol–water containing 2 g/l bioactive glass. FTIR studies showed that chitosan was absorbed on ceramic particle surface via hydroxyl and amid bonds. In order to evaluate the coating, its structure and electrochemical properties were studied. It was concluded that increasing the process voltage led to an increase in particle size and porosity, but induced cracks in the coating. In the presence of the polymer–bioactive glass coating, current density in artificial saliva was decreased by 52% and corrosion potential shifted toward more noble values.

© 2011 Elsevier Ltd and Techna Group S.r.l. All rights reserved.

Keywords: Implant; 316L stainless steel; Bioactive glass; Chitosan; Sol–gel; Electrophoretic

1. Introduction

Ceramic coatings on metallic substrates have many different applications, including biomedical ones where coatings are applied on implant's surface to improve its properties, and ameliorate its integration into the body [1]. Parameters which affect physical bonding and osseointegration of the implant include implant's corrosion resistance, crystal structure, surface morphology, as well as its design and application of proper surgical operations for placing it in the body.

In order to improve the bonding strength by formation of biological bonds between implant and bone [2], bioactive ceramics like hydroxyapatite and bioactive glass are deposited on the surface of the implant [3,4]. For a desirable orthopedic or dental implant, apart from biocompatibility, bioactivity is also an essential property. While bioactive glass and hydroxyapatite are both capable of bonding with their surrounding tissue, bioactivity of bioactive glass is higher than hydroxyapatite, since it has a

higher dissolution rate [5]. Moreover, the adherence of bioactive glass to the substrate is enhanced compared to hydroxyapatite, when sintered at similar temperatures [6]. Other advantages of these coatings include high chemical stability, strong bonding to the metallic substrate and the ability to tailor bioactive glass composition so that the thermal expansion coefficient of the coating and the substrate come close [7]. A thin hydroxycarbonate apatite (HCA) layer, which is the inorganic component of human bone, forms on bioactive glass coatings, when placed in biologic environment of the body [4,8]. Application of bioactive glass also improves the corrosion resistance of the substrate [9]. The major drawbacks of bioactive glass include low tensile strength, fatigue resistance and elastic modulus [10]. Therefore, bioactive glass coatings on metallic implants are recommended for orthopedic and dental applications to achieve a synergistic effect of bioactivity and mechanical strength [5]. Sol–gel is the most widely used technique for synthesis of bioactive glass. Sol–gel derived bioactive glass, compared to traditional melt processed, has higher bioactivity and biodegradability [11]. These properties are due to the nanoporous structure associated with sol–gel process. The high surface area of the sol–gel derived bioactive glass improves the rate of HCA layer formation and the ultimate bonding with host tissue [12–14].

^{*} Corresponding author. Tel.: +98 912 2470433; fax: +98 21 88080513.

E-mail addresses: mehdipour@mehr.sharif.edu (M. Mehdipour),
afshar@sharif.edu (A. Afshar).

The strength of the bonding between the coated implant and bone is an important factor in its service in the body. Moreover, the mechanical stability of the interface between coating and substrate is a significant factor during and after surgery. To improve these properties, different approaches have been examined. Heat treatment of the coating can increase strength of the coating's bonding to substrate [15]. However, sintering bioceramic coating at high temperatures degrades mechanical properties of the substrate [16]; therefore it is desirable that bioactive glass coatings with reasonable bonding and strength be applied on the substrate without sintering.

To achieve a coating with homogeneous mechanical properties, a composite structure is desirable and special attention has been given to the development of organic–inorganic composites by dispersing ceramic nanoparticles within a polymer matrix. Using composite coatings, polymeric phase bonds with substrate and thus the sintering step is avoided [17–19]. Different techniques such as plasma spray [20], sol–gel [21], sputtering techniques [22] and electrophoretic deposition (EPD) [6,23–26] have been employed to deposit bioactive glass coating on implant's surface. Advantages of electrophoretic deposition over other methods include low processing temperature, ability to form complex layers on substrates with intricate shapes, ability to control the thickness of the coating, simple equipment, low cost and high production rates [27,28]. EPD yields a homogeneous deposition with a uniform structure [29]. Chitosan is an interesting choice for electrophoretic deposition of composite coatings for its cationic nature in aqueous solutions and proper film forming properties [30].

The aim of this research is to coat a composite of bioactive glass and chitosan on a 316L stainless steel by EPD. Microstructure, chemical composition and functional groups of the surface of the bioactive glass and electrochemical behavior in artificial saliva are discussed.

2. Experimental

2.1. Materials and methods

Chitosan with molecular weight of 200 kDa and degree of deacetylation of about (85%), acetic acid, ethanol, tetra ethyl orthosilicate (TEOS), tetra ethyl phosphate (TEP), HNO_3 (65%), $\text{Ca}(\text{NO}_3)_2 \cdot 4\text{H}_2\text{O}$ and $\text{Mg}(\text{NO}_3)_2 \cdot 6\text{H}_2\text{O}$, were provided by Merck.

2.2. Synthesis of bioactive glass

$64\text{SiO}_2\text{--}26\text{CaO--}5\text{MgO--}5\text{P}_2\text{O}_5$ (mole%) bioactive glass was synthesized by hydrolysis of TEOS, TEP, $\text{Ca}(\text{NO}_3)_2 \cdot 4\text{H}_2\text{O}$, $\text{Mg}(\text{NO}_3)_2 \cdot 6\text{H}_2\text{O}$ and HNO_3 as catalyst. This solution is a slight modification by Saboori et al. [13] of that used for the first time by Li et al. [31]. TEOS was added to nitric acid solution (0.1 M) to give the desired bioactive glass composition and stirred for 30 min to allow complete hydrolysis of TEOS. TEP, $\text{Ca}(\text{NO}_3)_2 \cdot 4\text{H}_2\text{O}$ and $\text{Mg}(\text{NO}_3)_2 \cdot 6\text{H}_2\text{O}$ were added respectively

to the solution in 45 min intervals and the solution was stirred for an extra hour to assure completion of the reactions. It was then poured into a Teflon container, sealed and kept for 10 days at room temperature until completion of polycondensation reaction and gel formation. The gel container was kept for 24 h at 120 °C to dehydrate. It was also kept for 24 h at 700 °C to allow nitrate removal. To obtain a submicron powder, as-synthesized bioactive glass was grinded by a SPEX mill (Retsch Co., Germany; Model No. PM 200) for 4 h.

2.3. Electrophoretic deposition

316L stainless steel plates, 20 mm × 25 mm and 20 mm × 50 mm, were used as cathode and anode, respectively. The surface preparation included washing with distilled water, rinsing and degreasing by ultrasonic cleaning in acetone for 10 min and a final drying step. Bioactive glass powder of composition (wt%): 64% SiO_2 , 26% CaO , 5% MgO and 5% P_2O_5 and average particle size <1 μm was obtained.

Chitosan was dissolved in 1% acetic acid and was then used for preparation of the suspension for EPD. EPD was performed using 0.5 g/l chitosan solutions containing 2 g/l bioactive glass particles in different ratios of mixed ethanol–water solvent. Before EPD, the suspensions were ultrasonicated for 30 min to achieve a homogeneous dispersion of bioactive glass particles. The EPD cell for cathodic deposition included a 316L stainless steel cathode and anode. The distance between the cathode and the counter electrode was 10 mm. Deposition was performed at a constant voltage of 10–20 V cm^{-2} .

2.4. Characterization of the coating

2.4.1. FTIR studies

FTIR is a very useful method for identification of inorganic functional groups. FTIR was used to investigate the bonding of chitosan on bioactive glass particles. The deposited coating was scratched to prepare a sample for FTIR analysis. FTIR was performed using Perkin-Elmer RX1 in the wavenumber range of 400–4000 cm^{-1} and a resolution of 4 cm^{-1} .

2.4.2. Scanning electron microscopy

Morphology of the composite coating was examined using a scanning electron microscope (Philips, Holland; Model XL30). A thin section was taken from the coating and was Au sputtered about 10 nm thick prior to SEM analysis.

2.4.3. Electrochemical corrosion behavior

Bare and coated samples were studied for their electrochemical corrosion resistance in artificial saliva in room temperature. Artificial saliva was prepared according to the one proposed by Jean-Yves Gal et al. [32], the composition of which is given in Table 1. A three-electrode cell with a saturate calomel electrode (SCE), a working electrode (the sample) and a counter electrode (stainless steel) was employed. Polarization curves were obtained by Autolab (PGSTAT 362N) device with a scan rate potential set at 1 mV/s.

Table 1
Composition of the artificial saliva medium [32].

Compound	Concentration mg/l	Compound	Concentration mg/l
NaCl	125.6	Na ₂ SO ₄ ·10H ₂ O	763.2
KCl	963.9	NH ₄ Cl	178
KSCN	189.2	CaCl ₂ ·2H ₂ O	227.8
KH ₂ PO ₄	654.5	NaHCO ₃	630.8
Urea	200		

3. Results and discussion

3.1. Stability of chitosan–bioactive glass suspension

Mixed ethanol–water solvent was used to prepare chitosan–bioactive glass suspension. Chitosan does not dissolve adequately in pure ethanol and precipitates in high values of pH [23]. On the other hand, although water dissolves chitosan, but forms significant amounts of hydrogen gas on cathode's surface during EPD, which eventually leads to a porous coating. Increasing ethanol in ethanol–water solvent reduces the porosity by decreasing current density [17]. Thus, the goal is to reach an optimum ethanol–water ratio to obtain a uniform coating while maintaining a reasonable deposition rate. pH was measured before and after addition of 64SiO₂–26CaO–5MgO–5P₂O₅ bioactive glass powder and the results are given in Fig. 1.

As it can be seen in Fig. 1, pH decreases with increasing water ratio in ethanol–water solvent. Suspensions of 2 g/l bioactive glass powder in solvents with water ratios of less than 25% were unstable and the particles precipitated after about a minute. In these ratios pH reaches a value of 5.6, precipitating chitosan and ceramic particles [23]. Suspension of 2 g/l bioactive glass in solvent with 30% water was observed to be stable, having a pH of 5.22.

The conductivity of the suspension affects its stability. As shown in Fig. 2, increasing the water% increases the

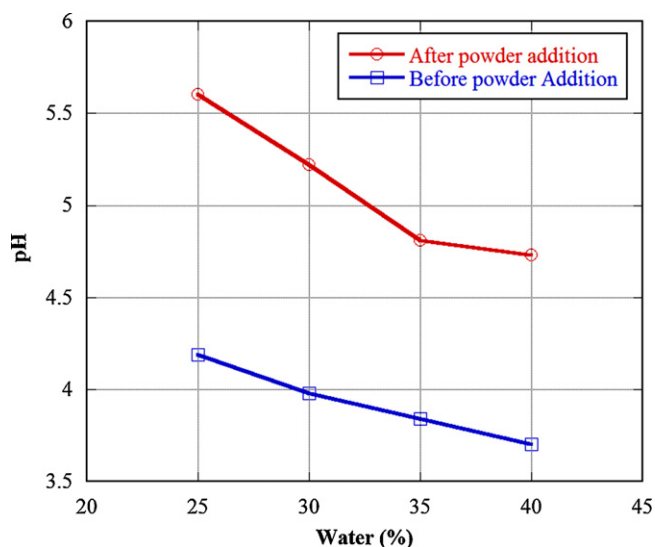


Fig. 1. The morphology of the composite coating was examined using a scanning electron microscope (Philips, Holland; Model XL30). A thin section was taken from the coating and was Au sputtered about 10 nm thick before SEM analysis.

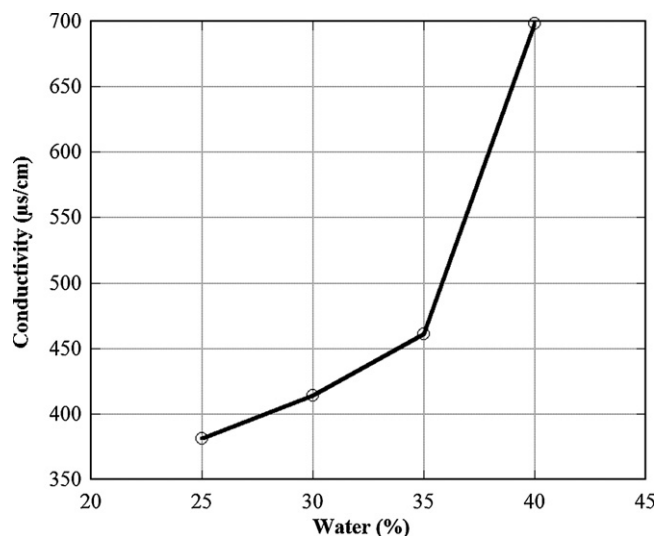


Fig. 2. The dependence of the water% in water–ethanol ratio on conductivity with 2 g/l bioactive glass.

conductivity of the suspension. Conductivity is highly related to ionic strength of the suspension. High ion concentrations in suspension lead to an increase in rate of agglomeration and the number of free ions. This large number of free ions may then act as principal current carriers, reducing speed of the particles and therefore the deposition rate [26]. Increasing water ratio from 30% to 40% reduced the coating's thickness from $12 \pm 2 \mu\text{m}$ to $6.1 \pm 2 \mu\text{m}$. Thus increasing water ratio increases conductivity and reduces the deposition rate, which is in accordance with the results of Wang et al. [26].

3.2. Characterization of the coating

The evolution of current density in 5 min of EPD is given in Fig. 3, for suspensions of 2 g/l bioactive glass in solvent with 30% water and in different EPD voltages. Current density lowers during EPD, the extent of which is larger at higher voltages. Polymer–ceramic coating acts as an insulating layer, reducing the effective electric field in the suspension, the applied force on

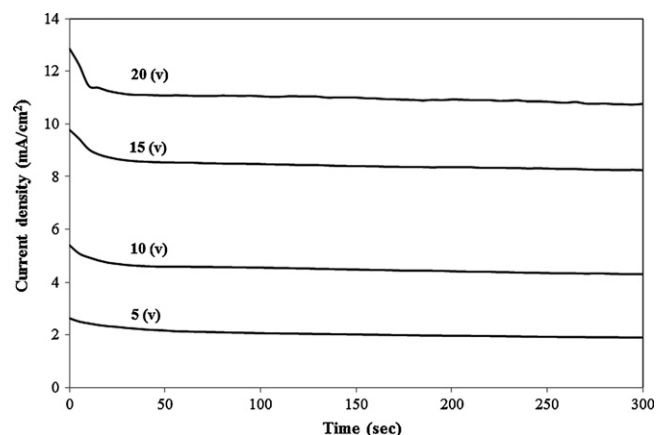


Fig. 3. Evolution of current density during EPD for suspensions of 2 g/l bioactive glass in solvent with 30% water in different EPD voltages.

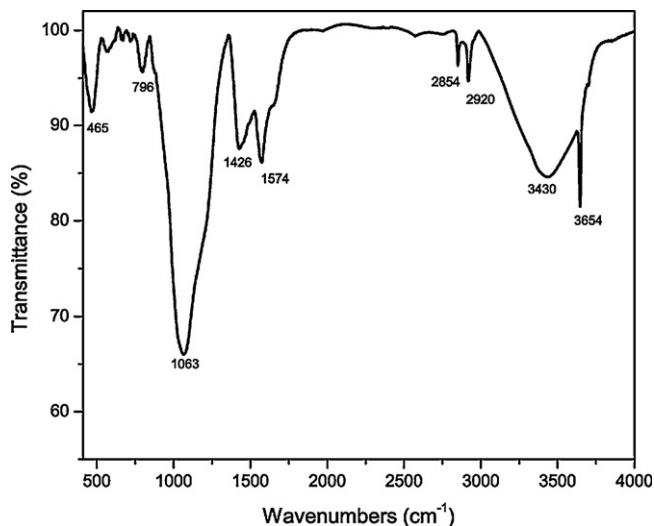


Fig. 4. FTIR spectra of bioactive glass ceramic with adsorbed chitosan.

the particles, particle movement toward electrode with opposite charge, and finally the current density [33].

For the particles to have good stability in the suspension, they require to have an electric charge on their surface (electrostatic repulsion mechanism) or form a layer on their surface as a physical barrier to agglomeration (steric mechanism) [27]. Thus, in both cases, particles need to be charged in order to improve particle stability and create a uniform coating.

Fig. 4 shows FTIR spectrum of the coating prepared in suspension with a water ratio of 30%. The bands at 463–468 cm^{-1} are assigned to P–O bonds of PO_4^{3-} group [34]; the bands at 796 cm^{-1} and 1063 cm^{-1} are related to Si–O–Si bonds of silicate group. The bands at 1426–1435 cm^{-1} are for the C–O bonds, and bands at 1487 cm^{-1} , 2854 cm^{-1} and 2920 cm^{-1} are for the C–H bonds of CH_2 and CH_3 groups. The band at 1574 cm^{-1} corresponds to N–H bonds of amide group and finally bands at 3430 cm^{-1} and 3654 cm^{-1} are assigned to O–H bonds of adsorbed water and structural hydroxyl group, respectively [35]. Castro et al. [36] suggested that the peaks for hydroxyl group at 3645 cm^{-1} , and adsorbed amide and methyl groups are characteristic of chitosan adsorption. Chitosan has long molecular chains, and when adsorbed on glass particles may act as a barrier to avoid agglomeration and therefore gives a highly stable suspension (steric mechanism) [27].

Structure of the coating was further studied by SEM. Chitosan from solution forms a matrix on the substrate where bioactive ceramic particles are dispersed into [37]. In fact, the polymer acts a binding intermediate between ceramic particles and metallic substrate which enhances coating's binding to the substrate.

As it is evident from Fig. 5, increasing EPD voltage causes more particles to be placed in the coating, covering the surface more thoroughly though with coarser particles. From Fig. 5, it could be understood that the coating prepared in EPD voltage of 10 V has less coarse agglomerates compared with the coatings applied in EPD voltages of 15 and 20 V; however the surface is not completely covered with glass particles. The SEM image of the coating prepared with EPD voltage of 20 V shows large

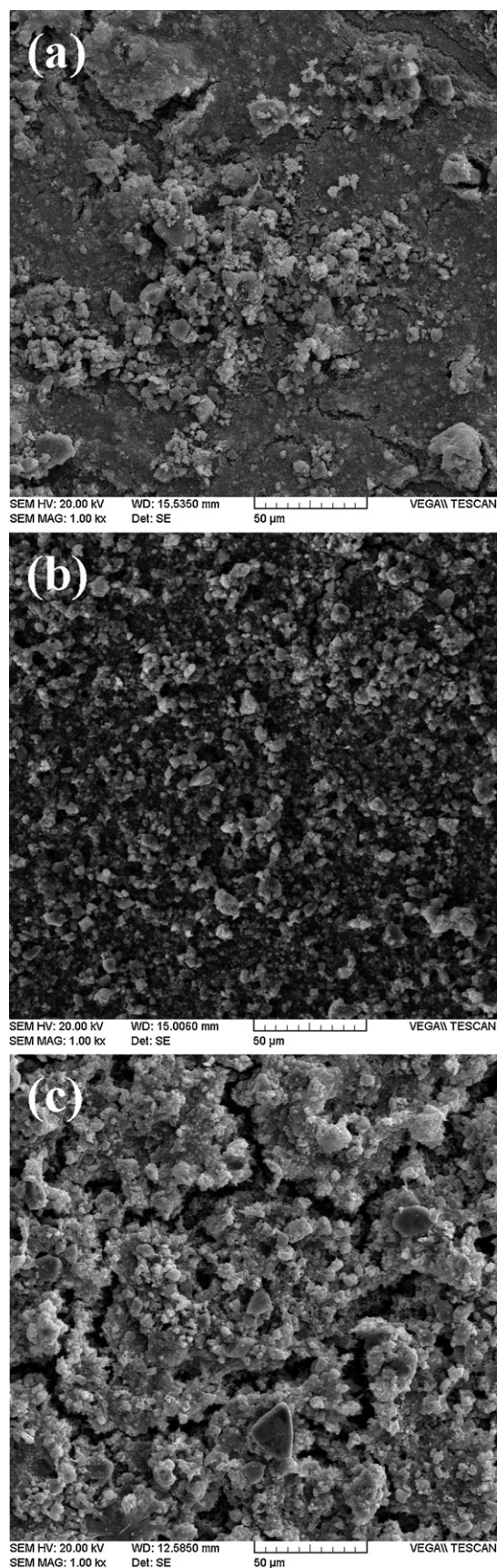


Fig. 5. SEM images of the surfaces of the deposits prepared from the 0.5 g/l chitosan solutions containing 2 g/l bioactive glass in constant time (a) 10 V, (b) 15 V and (c) 20 V.

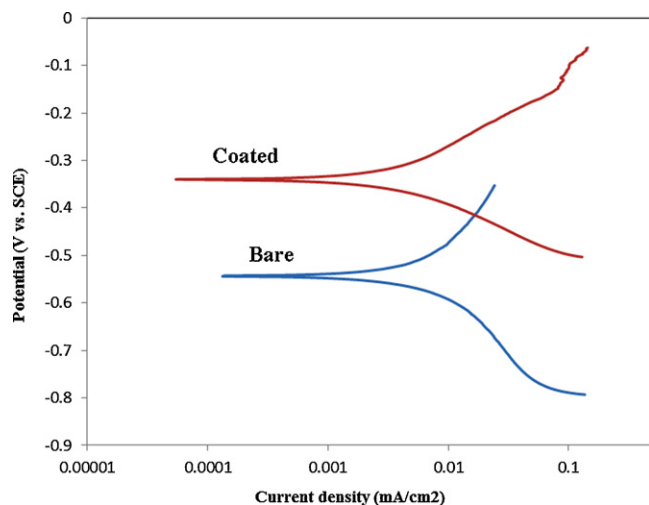


Fig. 6. polarization plots for the samples tested in artificial saliva solution for the bare and coated stainless steel.

numbers of coarse agglomerates and presence of cracks. For the coating prepared with EPD voltage of 15 V, a more uniform and yet crack-free surface was observed. It could thus be concluded that increasing EPD voltage increased the number of coarse agglomerated particles on the coatings surface. This is due to the fact that in low voltages, the electric field in the suspension is lower, leading to weaker induced forces which can only move particles with higher electrophoretic mobility. Increasing the voltage makes it possible to move agglomerated particles toward the coating's surface. Deposition of the coarser agglomerated particles on the coating's surface increases the coating's porosity [38]. It should be noted that the increase in porosity could be beneficial to the bonding of the implant to the surrounding tissue by increasing tissue ingrowth into the pores of the surface. On the other hand, porosity decreases the bonding between the coating and the substrate, increasing the corrosion rate of the implant. Hence an optimum porosity should be achieved by choosing the appropriate EPD voltage.

Fig. 6 shows polarization diagrams of 316L stainless steel with and without coating. Corrosion current density reduced by 52% from $6.97 \mu\text{A}/\text{cm}^2$ for the uncoated sample to $3.3 \mu\text{A}/\text{cm}^2$ for the coated sample. The chitosan–glass composite coating shifts polarization curve of the substrate to lower current densities and more noble potentials (from $-54 \pm 2 \text{ mV}$ to $-31 \pm 2 \text{ mV}$), which indicates the higher corrosion resistance of the coated 316L stainless steel in artificial saliva where the composite coating acts as a protective layer. These results are consistent with the findings of Pang and Zhitomirsky [17].

4. Conclusions

An electrochemical method was employed to coat a four component bioactive glass ($\text{SiO}_2\text{--CaO--P}_2\text{O}_5\text{--MgO}$)/chitosan composite on a 316L stainless steel substrate. This technique was based on electrophoretic deposition from mixed ethanol–water suspension of ceramic glass particles and chitosan. The influence of water to ethanol ratio on suspension stability was investigated and water ratio of 30% was found to yield a high

deposition rate and a uniform structure. FTIR results showed bands of O–H and N–H, characteristic of chitosan adsorption on particle surface. SEM investigations indicated formation of a uniform, smooth and crack-free coating on the substrate with a thickness of $7 \mu\text{m}$ for the sample prepared with EPD voltage of 15 V. The results of potentiodynamic polarization studies of the coated and uncoated samples in artificial saliva indicated that electrochemical corrosion parameters shifted toward more noble values in case of coated samples.

References

- [1] D.J. Trantolo, M.J. Yaszemski, K. Lewandowski, V. Hasirci, D.E. Altbelli, D.L. Wise, in: Macel Dekker, Inc, *Biomaterials in Orthopedics*, 2004, pp. 401–437.
- [2] Q.Z. Chen, C.T. Wong, W.W. Lu, K.M.C. Cheung, J.C.Y. Leong, K.D.K. Luk, Strengthening mechanisms of bone bonding to crystalline hydroxyapatite in vivo, *Biomaterials* 25 (18) (2004) 4243–4254.
- [3] Q.Z. Chen, I.D. Thompson, A.R. Boccaccini, *Biomaterials* 7 (11) (2006) 2414–2425.
- [4] L.L. Hench, *Journal of the American Ceramic Society* 1 (7) (1998) 1705–1728.
- [5] X.F. Xiao, R.F. Liu, *Materials Letters* 60 (21–22) (2006) 2627–2632.
- [6] A. Balamurugan, G. Balossier, J. Michel, J.M.F. Ferreira, *Electrochimica Acta* 4 (4) (2009) 1192–1198.
- [7] L. Peddi, R. Brow, R. Brown, *Journal of Materials Science: Materials in Medicine* 19 (9) (2008) 3145–3152.
- [8] F. Pishbin, A. Simchi, M.P. Ryan, A.R. Boccaccini, *Journal of the European Ceramic Society* 30 (14) (2010) 2963–2970.
- [9] J.B. Park, J.D. Bronzino, CRC Press, 2002.
- [10] R.D. Rawlings, *Clinical Materials* 4 (2) (1993) 155–179.
- [11] M.H. Fathi, A. Doostmohammadi, Bioactive glass nanopowder and bioglass coating for biocompatibility improvement of metallic implant, *Journal of Materials Processing Technology* 209 (3) (2009) 1385–1391.
- [12] Q.-Z. Chen, Y. Li, L.-Y. Jin, J.M.W. Quinn, P.A. Komisaroff, A new sol-gel process for producing Na_2O -containing bioactive glass ceramics, *Acta Biomaterialia* 6 (10) (2010) 4143–4153.
- [13] A. Saboori, M. Rabiee, F. Moztaazadeh, M. Sheikhi, M. Tahriri, M. Karimi, Synthesis, characterization and in vitro bioactivity of sol-gel derived $\text{SiO}_2\text{--CaO--P}_2\text{O}_5\text{--MgO}$ bioglass, *Materials Science and Engineering: C* 29 (1) (2009) 335–340.
- [14] Z. Hong, A. Liu, L. Chen, X. Chen, X. Jing, Preparation of bioactive glass ceramic nanoparticles by combination of sol-gel and coprecipitation method, *Journal of Non-Crystalline Solids* 355 (6) (2009) 368–372.
- [15] L. Lefebvre, J. Chevalier, L. Gremillard, R. Zenati, G. Thollet, D. Bernache-Assolant, A. Govin, Structural transformations of bioactive glass 45S5 with thermal treatments, *Acta Materialia* 55 (10) (2007) 3305–3313.
- [16] P. Fratzl, H.S. Gupta, E.P. Paschalis, P. Roschger, Structure and mechanical quality of the collagen–mineral nano-composite in bone, *Journal of Materials Chemistry* 14 (14) (2004) 2115–2123.
- [17] X. Pang, I. Zhitomirsky, Electrodeposition of composite hydroxyapatite–chitosan films, *Materials Chemistry and Physics* 94 (2–3) (2005) 245–251.
- [18] X.Z. Pang, I. Zhitomirsky, *International Journal of Nanoscience* 4 (2005) 409–418.
- [19] X. Pang, I. Zhitomirsky, Electrophoretic deposition of composite hydroxyapatite–chitosan coatings, *Materials Characterization* 58 (4) (2007) 339–348.
- [20] H. Herman, Plasma-sprayed coatings, *Scientific American (USA)* 259 (3) (1988) 112–117.
- [21] C. García, S. Céré, A. Durán, Bioactive coatings prepared by sol-gel on stainless steel 316L, *Journal of Non-Crystalline Solids* 348 (2004) 218–224.
- [22] J.K. Bibby, N.L. Bub, D.J. Wood, P.M. Mummery, Fluorapatite–mullite glass sputter coated Ti6Al4V for biomedical applications, *Journal of Materials Science: Materials in Medicine* 16 (5) (2005) 379–385.

- [23] D. Zhitomirsky, J.A. Roether, A.R. Boccaccini, I. Zhitomirsky, Electrophoretic deposition of bioactive glass/polymer composite coatings with and without HA nanoparticle inclusions for biomedical applications, *Journal of Materials Processing Technology* 209 (4) (2009) 1853–1860.
- [24] D. Krause, B. Thomas, C. Leinenbach, D. Eifler, E.J. Minay, A.R. Boccaccini, The electrophoretic deposition of Bioglass[®] particles on stainless steel and Nitinol substrates, *Surface and Coatings Technology* 200 (16–17) (2006) 4835–4845.
- [25] A. Boccaccini, C. Peters, J. Roether, D. Eifler, S. Misra, E. Minay, Electrophoretic deposition of polyetheretherketone (PEEK) and PEEK/Bioglass[®] coatings on NiTi shape memory alloy wires, *Journal of Materials Science* 41 (24) (2006) 8152–8159.
- [26] C. Wang, J. Ma, W. Cheng, R. Zhang, Thick hydroxyapatite coatings by electrophoretic deposition, *Materials Letters* 57 (1) (2002) 99–105.
- [27] L. Besra, M. Liu, A review on fundamentals and applications of electrophoretic deposition (EPD), *Progress in Materials Science* 52 (1) (2007) 1–61.
- [28] A.R. Boccaccini, I. Zhitomirsky, Application of electrophoretic and electrolytic deposition techniques in ceramics processing, *Current Opinion in Solid State and Materials Science* 6 (3) (2002) 251–260.
- [29] T.M. Sridhar, U. Kamachi Mudali, M. Subbaiyan, Preparation and characterisation of electrophoretically deposited hydroxyapatite coatings on type 316L stainless steel, *Corrosion Science* 45 (2) (2003) 237–252.
- [30] A. Simchi, F. Pishbin, A.R. Boccaccini, Electrophoretic deposition of chitosan, *Materials Letters* 63 (26) (2009) 2253–2256.
- [31] R. Li, A.E. Clark, L.L. Hench, An investigation of bioactive glass powders by sol–gel processing, *Journal of Applied Biomaterials* 2 (4) (1991) 231–239.
- [32] J.-Y. Gal, Y. Fovet, M. Adib-Yadzi, About a synthetic saliva for in vitro studies, *Talanta* 53 (6) (2001) 1103–1115.
- [33] I. Zhitomirsky, L. Gal-Or, Electrophoretic deposition of hydroxyapatite, *Journal of Materials Science: Materials in Medicine* 8 (4) (1997) 213–219.
- [34] S. Koutsopoulos, Synthesis and characterization of hydroxyapatite crystals: a review study on the analytical methods, *Journal of Biomedical Materials Research* 62 (4) (2002) 600–612.
- [35] C. Paluszkiwicz, E. Stodolak, M. Hasik, M. Blazewicz, FT-IR study of montmorillonite–chitosan nanocomposite materials, *Spectrochimica Acta Part A: Molecular and Biomolecular Spectroscopy* 79 (2011) 784–788.
- [36] R.H.R. Castro, D. Gouvêa, The influence of the chitosan adsorption on the stability of SnO₂ suspensions, *Journal of the European Ceramic Society* 23 (6) (2003) 897–903.
- [37] A.R. Boccaccini, S. Keim, R. Ma, Y. Li, I. Zhitomirsky, Electrophoretic deposition of biomaterials, *Journal of The Royal Society Interface* 7 (Suppl 5) (2010) S581–S613.
- [38] I. Zhitomirsky, Cathodic electrodeposition of ceramic and organoceramic materials. Fundamental aspects, *Advances in Colloid and Interface Science* 97 (1–3) (2002) 277–315.